Published in final edited form as:
Cancer Prev Res (Phila). 2012 May ; 5(5): 706–716. doi:10.1158/1940-6207.CAPR-11-0508.

Programmable Bio-Nano-Chip Systems for Serum CA125 Quantification: Towards Ovarian Cancer Diagnostics at the Point-of-Care

Archana Raamanathan[1,2], **Glennon W. Simmons**[1], **Nicolaos Christodoulides**[1], **Pierre N. Floriano**[1], **Wieslaw B. Furmaga**[3], **Spencer W. Redding**[4], **Karen H. Lu**[5], **Robert C. Bast Jr.**[6], and **John T. McDevitt**[1]

[1]Departments of Bioengineering and Chemistry, Rice University, Houston, TX

[2]Department of Chemistry and Biochemistry, The University of Texas at Austin, Austin, TX

[3]Department of Pathology, University of Texas Health Science Center at San Antonio, San Antonio, TX

[4]Department of Dental Diagnostic Science, University of Texas Health Science Center at San Antonio, San Antonio, TX

[5]Department of Gynaecologic Oncology, The University of Texas, MD Anderson Cancer Center, Houston, TX

[6]Department of Experimental Therapeutics, The University of Texas, MD Anderson Cancer Center, Houston, TX

Abstract

Point-of-care (POC) implementation of early detection and screening methodologies for ovarian cancer may enable improved survival rates through early intervention. Current laboratory-confined immunoanalyzers have long turnaround times and are often incompatible with multiplexing and POC implementation. Rapid, sensitive and multiplexable POC diagnostic platforms compatible with promising early detection approaches for ovarian cancer are needed. To this end, we report the adaptation of the programmable bio-nano-chip (p-BNC), an integrated, microfluidic, modular (*Programmable*) platform for CA125 serum quantitation, a biomarker prominently implicated in multi-modal and multi-marker screening approaches. In the p-BNC, CA125 from diseased sera (*Bio*) is sequestered and assessed with a fluorescence-based sandwich immunoassay, completed in the nano-nets (*Nano*) of sensitized agarose microbeads localized in individually addressable wells (*Chip*), housed in a microfluidic module, capable of integrating multiple sample, reagent and biowaste processing and handling steps. Antibody pairs that bind to distinct epitopes on CA125 were screened. To permit efficient biomarker sequestration in a 3-D microfluidic environment, the p-BNC operating variables (incubation times, flow rates and reagent concentrations) were tuned to deliver optimal analytical performance under 45 minutes. With short analysis times, competitive analytical performance (Inter- and intra-assay precision of *1.2%* and *1.9%* and LODs of *1.0 U/mL*) was achieved on this mini-sensor ensemble. Further validation with sera of ovarian cancer patients (*n=20*) demonstrated excellent correlation ($R^2 = 0.97$) with gold-standard ELISA. Building on the integration capabilities of novel microfluidic systems programmed for ovarian cancer, the rapid,

Corresponding Author: John T. McDevitt, Departments of Bioengineering and Chemistry, Rice University, 6100, Main Street, MS 142, Houston, TX 77005. Fax: 713-348-2302; Phone: 713-348-2123; mcdevitt@rice.edu.

Disclosure of Potential Conflicts of Interest: J. T. McDevitt: ownership interest and consultant/advisory board, LabNow; R.C. Bast, Jr.: Receives royalties for CA125 and serves on the scientific advisory board for Fujirebio Diagnostics, Inc. The other authors declare no potential conflict of interest.

precise and sensitive miniaturized p-BNC system shows strong promise for ovarian cancer diagnostics.

Keywords

Programmable Bio-Nano-Chip; Serum CA125; Point-of-Care; Microfluidics; Ovarian Cancer; Early Detection; Lab-on-a-Chip

Introduction

In 2010, approximately 21,880 women will be diagnosed with ovarian cancer in the United States and 13,850 women will succumb to this disease (1). Although 90% of ovarian cancers can be treated at stage I with the currently existing surgical and chemotherapeutic regimens, only 25% of ovarian cancers are detected at this treatable stage due to the non-specific symptoms and the lack of effective screening procedures (2-4). Given the low prevalence of ovarian cancer (1 in 2500 post menopausal women), an extremely high specificity (99.6%) and sensitivity (> 75%) are required to achieve a minimum positive predictive value (PPV) of 10% (i.e. 10 laparotomies per case of ovarian cancer detected) (5). No screening test exists currently for recommended use in the general population, underscoring the need for novel early detection and easily completed screening methods (6).

For suspected pelvic masses, ovarian cancer diagnosis is realized by pelvic examination, transvaginal sonography (TVS) and serum CA125 leading to exploratory or diagnostic laparoscopy (4). TVS provides a precise image of the ovary and while PPVs in the most promising studies have been reported to be close to 10%, prohibitively high costs for implementation has precluded its utility as a first line screen (2, 7, 8).

The biomarker CA125 is a heavily glycosylated high MW protein encoded by the MUC16 gene with a potential role in contact and adhesion for metastasizing epithelial ovarian cancer cells (9, 10). The extracellular domain shed in serum from the surface of the ovarian cancer cells following cytoplasmic phosphorylation and proteolytic cleavage is elevated in 80% of advanced stage carcinomas (11, 12). Hence, serum CA125 has been extensively utilized and has been FDA approved for recurrent disease detection and monitoring chemotherapy response (13). However, CA125 is elevated in only 50-60% of early stage cancers with false positives for a variety of non-malignant gynecological and physiological conditions (14, 15).

The inaccessibility of the ovaries for screening has generated extensive interest in non-invasive serum biomarker based methodologies for first line screens and two approaches are being investigated. In multi-modal screening, the patient's risk for ovarian cancer is stratified by monitoring longitudinal values of CA125, interpreted with a Risk of Ovarian Cancer Algorithm (16, 17). Based on assessed risk levels, patients are triaged for follow-up with CA125, TVS or surgery (18). In an ongoing, large, randomized controlled trial of 202,638 women (UKCTOCS), the MMS showed promising PPVs of 43.3% (19). Nevertheless, 20% of ovarian cancers do not express CA125 and in multi-marker panel screening, multiple biomarkers taken together as a panel, have shown improved sensitivity and specificity compared to CA125 alone (2, 20, 21). Such biomarkers have been identified with proteomic techniques (22, 23), with the most promising panels comprising 3-4 biomarkers, presented as complementary to CA125 (24, 25).

The POC implementation of aforementioned biomarker-based early detection and screening methodologies may potentially impact survival rates through early intervention with increased access to rapid, low-cost, large-scale population screening. Aligned with

promising research, such diagnostic platforms programmed for ovarian cancer should entail multiplexability, high quality analytical performance (precision and sensitivity) and sample economy. Multiplexability and sample economy are crucial for validation of multi-marker panels discovered by proteomic techniques with limited supply of early stage preclinical samples (26, 27). Further, longitudinal monitoring of CA125 and other biomarker levels necessitate high precision to discern biological variations and low limit of detection to facilitate early disease detection (28). Finally, rapid analysis times will permit immediate access to TVS, when required and minimize follow-up visits, with additional advantages of reduced patient discomfort and anxiety. A multi-functional diagnostic platform that can be utilized for assay development and validation and in turn can function as the end-point diagnostic will significantly reduce residence time in the 'diagnostic pipeline paradigm' enabling speedier translation of biomarkers from discovery to diagnostics (23). Current gold standard methodologies such as ELISA, dependent on centralized laboratory infrastructure, have typical turnaround times on the order of 24-48 hours (29). Further, the single marker at a time approach and the need for trained personnel are inconducive for multiplexing and POC implementation (29, 30). While flow cytometric bead-based approaches tackle the issue of multiplexing and have served well for biomarker discovery, other technological constraints remain similar (31).

Microfluidic platforms have been proposed for POC applications in cancer diagnostics due to their inherent advantages of low cost, sample and reagent economy, low detection limits, rapid analysis times, portability, automation and ease of operation by non-expert users (29). However, to realize widespread distribution, highly application-oriented systems tailored to address specific analytical and research needs of the pertinent clinical community (as discussed earlier for ovarian cancer) are needed (32). Unfortunately, technological maturation of microfluidic platforms has not complemented advances in cancer biomarker discovery attributable to the apparent disconnect between the relevant communities, crucially important for this highly inter-disciplinary translational effort (33). In terms of technological constraints, reliance on centralized laboratory infrastructure akin to conventional immunoanalyzers, need to be overcome through miniaturized 'analyzer' components to supplement the microfluidic device (34). Though an instrument-free setup would be preferred, high sensitivity quantitative analysis for ovarian cancer biomarkers necessitates optical detection and consequently, miniaturized optical and mechanical components for POC implementation (35). Following sample input, all subsequent processes need to be automated with minimal user interaction in a closed format suitable for biohazardous material handling (29).

Rapid, reliable, and efficient measurement of multiple key biomarkers simultaneously at the POC has the potential to transform clinical laboratory science. Toward this goal, the McDevitt laboratory has sustained efforts to improve POC *in vitro* diagnostics, through the development, validation and implementation of Programmable Bio-Nano-Chips (p-BNC) (36, 37). The **programmable** feature of these systems refers to the capacity of the sensor ensemble to function as a standard platform that can be retasked (i.e. programmed) to serve a new application through insertion of molecular level code (i.e. the biomarker-specific reagents). The **Bio** terminology relates to the capacity to measure and extract the bio-signatures associated with disease progression. The **Nano** element describes the capacity to miniaturize the system, embodied in the use of nano-nets for efficient and rapid biomarker capture as well as quantum dots for increased signal generation. The **chip** term emphasizes the capacity to mass-produce the sensor elements in ways analogous to those used by the microelectronics industry. In this work, we report our initial efforts to customize the p-BNC system, to address specific needs in ovarian cancer biomarker-based screening, utilizing CA125 as the proof-of-concept biomarker. Here, we explore critical variables pertaining to reagent screening and assay development in a microfluidic environment, that serve to

influence the analytical performance of the mini-sensor ensemble under time constraints imposed for POC applications. This report further details CA125 quantitation in advanced stage ovarian cancer patient sera and validation against gold standard platforms, and explores the potential of the p-BNC system in the context of MMS and MMP screening strategies.

Materials and methods

Immunoreagents and buffers

All reagents utilized for performing immunoassays in the p-BNC were prepared in PBS (Thermo Fisher Scientific) containing 0.1% (w/v) BSA (Sigma Aldrich) needed for reagent stability and blocking non-specific binding (PBSA). Anti-CA125 monoclonal antibodies (Clones M002201, M002203, M77161, M8072320, M8072321 and M8072322) were obtained from Fitzgerald Industries International. Low cross-reactivity, calibrator grade CA125 standards were acquired from Meridian Life Science. Human serum based Liquicheck® tumor marker controls were procured from BioRad for precision studies.

p-BNC construction and assay execution

The various generations of p-BNC were fabricated utilizing xurography based rapid prototyping techniques. Technical details regarding construction are provided in the supplementary information section.

A typical assay was executed with analyte specific beads and negative control beads (IL-6) localized in the individually addressable wells on the chip housed in the p-BNC microfluidic ensemble. Alternatively, beads of varying concentrations or antibody clones were multiplexed along adjoining columns and identified by location for optimization studies. Following a 1 minute high flow rate step (2500 μL/min) for priming and microbubble elimination, the serially diluted analyte of pre-determined concentration in PBSA or the serum sample was introduced to the bead array. Any remaining uncaptured analyte following this step, was removed with a high stringency, high flowrate PBS wash. The immunosandwich was completed in the agarose nano-nets with the introduction of Alexa Fluor® 488 conjugated detecting antibody, followed by removal of excess antibody with a high stringency wash and digital image capture of the fluorescent beads to quantify the captured analyte.

CA125 ELISA

ELISAs were performed at MD Anderson Cancer Center (MDACC) and University of Texas, Heath Science Center at San Antonio (UTHSCSA) with standard manufacturer protocols (Elecsys CA125 II electrochemiluminescence assay on the ‘cobas e’ immunoanalyzer, Roche diagnostics).

Sample collection and analysis

Serum samples were collected from advanced stage (III and IV) ovarian cancer patients with informed consent following IRB approved procedures at MDACC *(n=10)* and UTHSCSA *(n=10)* using routine protocols (See supplementary information). The aliquoted samples were analyzed by ELISA at the collection institutions and sent to the McDevitt laboratory over dry ice for analysis on the p-BNC.

Image analysis

Images obtained were analyzed utilizing open-source ImageJ (NIH) software with custom image analysis macros to yield the mean fluorescence intensity (MFI) for the corresponding

area of interest (AOI) on the beads (38). Further details are provided in the supplement section.

Statistical analysis

Calibration curves were generated using SigmaPlot 10 (SPSS Inc) and fitted to a four parameter logistic equation. Linear regression, determination of unknown concentrations from standard curves and curve fitting were performed utilizing the same software. Precision analysis was performed via the methods analysis module of Microsoft Excel. All optimization experiments were conducted in triplicate and error bars denote inter-assay precision unless otherwise noted.

Results

Programmable bio-nano-chip systems at the point-of-care

The programmable bio-nano-chip (p-BNC) system (Fig. 1) is a highly sensitive, multiplexable, POC amenable microfluidic platform consistent with requirements set forth for the next generation of ovarian cancer diagnostic devices (see introduction). This mini-sensor ensemble consists of two main parts: a disposable cartridge that contains the programmable chip module and portable instrumentation that serves as the user interface, thereby reading, analysing, storing data and reporting the results. This system is suitable for point of service quantitation of CA125 and expanded multiplexed panels that may be completed with finger-stick quantities of blood.

The completely integrated p-BNC (Fig. 2A, III) is composed of modular sub-assemblies, built around a micromachined stainless steel bead holder chip housing the programmable agarose microbead ‘immunoanalyzer’ core, sandwiched in a plastic microfluidic card, that integrates various on-card fluid handling processes, a sample input port and reagent containing blister packs. The programmable microbead immunoanalyzer core is identical between various generations of the p-BNC (Fig. 2A, I, III) and is capable of high efficiency analyte capture in a 3D agarose nano-net (Fig. 2B, III), sequestered from biological matrices to aid rapid, ultra-sensitive quantitative measurements of disease biomarkers in a fluorescence-based sandwich immunoassay format (Fig. 2C, I-IV). The integrated microfluidic assemblage contains a sample loop with an overflow chamber for precise on-card sample metering, in-line filters and selectively permeable membranes for debris and bubble removal, reagent pads and blister packs for on-card reagent and buffer storage, in-line micromixers for uniform reagent delivery to the immunoanalyzer core and an on-card waste disposal chamber (Fig. 2A, III). Efforts from our translational partners have led to the development of a miniaturized analyzer (Fig. 1) with scaled down light emitting diode-based optics, a miniaturized microscope and camera, battery powered source and linear actuated stepper motors to crush the blister packs and to release buffer and reagents to drive the immunoassay to completion, followed by optical detection and output. These significant advances when fully developed and placed into widespread clinical practice have the potential to permit untethering from laboratory supplies such as pipettes, reagent and buffer cold-chain, microscopes and pumps, limitations associated with the traditional laboratory infrastructure (Fig. 2A, I) to realize the POC potential of the p-BNC.

Here, we focus on the adaptation of the immunoanalyzer module of the p-BNC for rapid, sensitive and precise quantification of serum CA125, as the proof-of-concept biomarker for ovarian cancer, with prominent implications in the multi-modal and multi-marker screening strategies, in order to derive the technical and operational specifications for the clinical-grade p-BNC.

Optimization of p-BNC operating variables

Like ELISA, the p-BNC system utilizes sandwich immunoassays (Fig. 2C); however, immunocomplexes are formed throughout the 3-dimensional (3D) bead matrix (Fig. 2B, III), rather than on a 2D flat surface in ELISA. Here, the p-BNC enhanced dimensionality in a dynamic (i.e., non-equilibrium) microfluidic environment yields new challenges related to assay development and optimization. Efficient biomarker capture translating into high performance immunoassays is influenced by a complex interplay of operating variables: epitope guided matched pair screening, matched pair orientation, capturing and detecting antibody concentrations, sample and detecting antibody incubation times and the flow rates corresponding to these incubation steps. Hence, these variables were individually assessed to derive optimal matched pairs and operating conditions (technical specifications) based on analytical performance criteria (slope, Limit Of Detection (LOD), precision and linearity).

Matched antibody pair selection

The extracellular domain of CA125 shed in serum has multiple 156 amino acid repeat domains, each containing the 3 major non-overlapping epitopes recognized by the OC125-like, M11-like and OV197 antibodies (10, 39). Based on this established epitope mapping data, an array of antibodies were chosen to encompass the 3 distinct domains on the molecule; OC125-like antibodies (clones M002201 and M8072320); M11-like antibodies (clones M77161, M80272321 and M002203) and OV197-like antibody (clone M8072322). The matched pair identification for the CA125 sandwich immunoassay was enabled by screening each of the aforementioned clones in both capturing and detecting formats, thus potentially testing 30 such combinations.

‘Non-restrictive conditions’ involving 30 minute incubation times for both the analyte and detecting antibody to permit sufficient reaction times at slow flow rates (250 μl/min), a flow-through format to avail excess analyte, relatively high analyte (100, 250 and 500 U/mL) and detecting antibody concentrations (1:250 dilution) to ensure adequate signal visualization were utilized to enable matched pair identification under unoptimized conditions. A small subset of the results from this extensive study is presented in Fig. 3A encompassing the matched pair selected eventually. Here M8072320 (OC125) was chosen as the detecting antibody and the results (MFI against CA125 concentrations) represent the performance of the other 5 clones as capture antibodies immobilized on the agarose microbeads (107 ng/bead concentration) to form a matched pair for CA125.

The performance gradient of the various antibody pair combinations was concordant with expectations based on epitope specificities. Antibodies binding to the same domain and from the same clone performed the poorest (M8072320 capture and detection) represented by a relatively flat response in Fig. 3A and served as the negative control with the lowest slope and SNR (signal-to-noise ratio) at lowest tested concentration. The antibodies recognizing the same epitope, but from different clones (M002201 capture and M8072320 detection) exhibited poor, albeit slightly improved response above negative control, suggestive of strong competition between the clones for the same epitope. The other matched pairs formed between the detecting antibody (M8072320 – OC125) with other capture antibodies recognizing distinctly different domains (M11 and OV197) demonstrated good response over the tested range, with the performance gradient based on relative antibody affinities. M8072320 (OC125) clone for detection paired with M8072321 (M11) clone as the capture antibody exhibited the best performance in terms of aforementioned performance parameters with the highest slope, SNR and linearity among the 30 tested combinations.

The assignment of the capturing and detecting antibody orientation for a given matched pair is critical to the p-BNC performance as illustrated by Fig. 3B. Here, a matched pair formed

with the optimal 'correct orientation' performed significantly better in comparison to the 'reverse orientation' where the capturing and detecting moieties were interchanged, in contrast to results reported in the literature for flow cytometric bead based immunoassays and ELISAs for identical clones (40). Further, microfluidic immunosensors such as the p-BNC operate under dynamic (i.e. non-equilibrium) conditions in contrast to the aforementioned systems, necessitating extensive screening to arrive at optimal matched pairs and orientation as elucidated by this study (40, 41).

Concomitant optimization of immunoreagent concentrations

To avoid pre-biasing based on order of optimization, the capturing and detecting reagent concentrations were optimized concomitantly. 'Non restrictive' incubation times and flow rates as previously described were utilized. Agarose microbeads with 320, 107 and 5 ng/bead immobilized capturing antibody concentrations were multiplexed via spatial recognition along each column (3 × 4 array), permitting simultaneous exploration of multiple reagent concentrations and calibration curves were generated with various detecting antibody dilutions (1:250, 1:500 and 1:1000). Representative photomicrograph from this study at 50 U/mL CA125, 1:250 detecting antibody dilution and various tested capturing antibody concentrations is presented in Fig. 4A.

A 3-D surface plot was generated to simultaneously assess the effects of capturing and signalling antibody concentrations on the slope of the calibration curve (Fig. 4B). The slope was the highest with a capturing antibody concentration of 320 ng/bead at 1:250 detecting antibody dilution, but at the cost of linearity ($R^2 = 0.7345$). The effect of capturing antibody concentration on the slope at the optimal detecting antibody concentration (exhibiting the highest linearity) is depicted in Fig. 4C. The upper and lower bounds for exploring detecting antibody dilutions were set on the basis of deviation from linearity at the upper end and unacceptably low SNR at the lower end. Similarly, concentrations lower than 5 ng/bead of capturing antibody provided unacceptably low SNR and concentrations higher than 320 ng/bead did not offer any additional analytical advantages. This behaviour is indicative of either the loading capacity of the beads or lack of diffusion into porous beads and access to the additional binding sites (generated with increased capture antibody concentration) due to steric hindrance resulting from the size of CA125. The optimal capturing and detecting antibody concentration combination with the highest linearity ($R^2 = 0.999$) along with the maximum SNR and slope were chosen as 320 ng/bead and 1:500 dilution respectively for further experimentation.

Influence of flow rates and incubation times

The flow rate/time dependence of reagent and sample delivery was explored to identify if these crucial determinants can be tuned to practical time constraints, without loss of performance. As such, upper limit for the total assay time for the optimization steps described previously was set at a maximum of one hour. Detecting antibody reagents have lower volume restrictions in comparison to serum samples and hence the corresponding incubation time was chosen first for optimization. With previously chosen optimal matched pairs and reagent concentrations, incubation times were varied from 10 to 30 minutes under equimolar conditions (to preclude bias from lower reagent availability). Longer incubation times resulted in poor assay performance in terms of low slope and SNR along with high imprecision (Fig. 5A). Given that the detection step follows analyte capture by the immobilized capturing antibody (Fig. 2C, III), shorter incubation times are sufficient to complete the immunosandwich as indicated by this data. Longer incubation times and slower flow rates correspond to excess detecting antibody in the pores necessitate higher wash times to discard the unbound reagent. However, wash times and wash flow rates were held constant in this study leading to the pronounced effect of longer incubation times on the

slope and precision. Further given the molecular size of CA125, analyte capture is realized mainly on the periphery of the bead (Fig. 4A) enabling the detecting reagent easy access and fostering shorter incubation times. Consequently, a detecting antibody incubation time of 10 minutes was chosen as optimal, as improvements in slope and precision resulting from lowering incubation times levels off at this time.

The sample incubation was carried out under the closed loop 'recirculation mode' to increase analyte exploitation. A flow rate range of 250 μL/min to 1500 μL/min was examined, translating into 7.5 to 45 passes (repeated introduction of the sample) to the array and the corresponding effect on slope is documented in Fig. 5B. The slope rises steeply with increase in flow rate reaching a maximum at 750 μL/min and then levels off. Initial increase in the slope can be attributed to overcoming transport limitations and consequently improved analyte exploitation, a frequently encountered situation in microfluidic systems (42). Beyond 750 μL/min, the reaction limited regime prevails and hence improvements in slope level off at this time (43). The optimal flow rate was selected as 750 μL/min. Similar trends were observed for lower immobilized concentrations albeit at different optimal 'cut-off' flow rates (Fig. 5B). The corresponding incubation time was held at 30 minutes as any further decrease resulted in unacceptably low SNR (data not shown). The CA125 p-BNC immunoassay conducted with the optimal parameters was completed in a total of 43 minutes inclusive of wash times making it ideally suited for implementation in a POC setting.

The LOD following each optimization step along with the corresponding linearity and %CV is tabulated (Table 1). These results indicate performance improvement in terms of LOD with each step, with the most increase noted for the sample incubation flow rate optimization step. This is expected as this step leads to increased analyte exploitation and is consistent with previous studies (44). Immunoassay variables interact in a complex manner with each other and the iterative approach presented here cannot account for these interactions and is subject to bias from the order of optimization steps. A statistical design of experiments method is currently being explored to address this issue.

Analytical validation

Utilizing the optimized CA125 immunoassay, standard curves were obtained over the range of 10-400 U/mL, pertinent to early disease detection. The calibration curve was linear (R^2 = 0.99) over this range and the corresponding dose-response curve fitted to a four parameter logistic equation is shown in Fig. 6A.

The zero analyte concentration was evaluated in triplicate and the concentration corresponding to three standard deviations above the mean signal at zero was determined as the LOD. The LOD of 1.0 U/mL was comparable to the values reported (0.05 to 1.45 U/mL range) for the currently available commercial systems (45).

To evaluate precision, serum based tumor marker control standards corresponding to low (21.1 U/mL), medium (64.2 U/mL) and high (186 U/mL) concentrations were utilized. The intra-assay precision of the p-BNC, denoting the variation between the analyte sensitized beads placed within a chip (6 of 9 beads considered), was evaluated for these 3 standards. The inter-assay precision between the chips was estimated for the 3 standards over 3 consecutive days. For the low, medium and high standards, the intra-assay precision (%CV) values were 1.4, 3.0 and 1.3%, respectively, and the inter-assay precision (%CV) values were 1.2, 1.5 and 0.82%, respectively. The precision values obtained on the mini-sensor ensemble were competitive with current commercial lab-based standards (45). The slightly higher intra-assay precision is reflective of bead sensor homogeneity and uniform fluid delivery. Further, the automated p-BNC minimizes assay variations resulting in excellent inter-assay precision. Finally, potential interference from serum components were ruled out

due to dilution linearity (R^2 = 0.98) tested for a pre-selected serum sample with a high CA125 value (data not shown).

Method validation

To demonstrate clinical utility of the p-BNC, CA125 levels were assessed in sera obtained from advanced stage ovarian cancer patients *(n=20)*. Sera (100 μl) were diluted ten-fold with 0.1% PBSA and CA125 values were determined from standard calibration curves on the p-BNC. Accounting for differences in calibrators between the methods, the results from this study are presented in Fig. 6B. The concentrations obtained on the p-BNC correlated well with the current FDA approved gold standard ELISA (R^2=0.97). Samples with CA125 > 4000 U/mL were analyzed, but excluded from the results presented here due to the limited number of data points in the region.

Discussion

The p-BNC synergizes components from microfluidics, biomarker discovery, clinical chemistry and image analysis and in this work, we have adapted the miniaturized integrated immunoanalyzer for specific applications in ovarian cancer diagnostics. The p-BNC harnesses inherent microfluidic advantages of reduced assay times, reagent and sample economy upon multiplexing and inexpensive construction; along with multiplexability and POC amenability compliant with requirements for novel early detection and screening platforms for ovarian cancer.

We chose CA125 as the proof-of-concept biomarker due to its prominent implications in the MMS and MMP strategies. For optimal matched pair identification, we investigated 30 antibody pair combinations and qualified them based on rigorous analytical response criteria for the highest immunoassay slope, linearity and precision along with the lowest LOD (Fig. 3A, B). We delineated and optimized the variables affecting p-BNC performance; reagent concentrations (Fig. 4B, C), sample and reagent incubation times (Fig. 5A) and the corresponding flow rates (Fig. 5B). We tapped the multiplexing potential of the p-BNC to simultaneously analyze multiple antibody clones and reagent concentrations on a single microchip (Fig. 4A). Each optimization step resulted in qualified improvement based on analytical response criteria (Table 1). The LOD (1.0 U/mL) and the inter- and intra-assay precision (1.2% and 1.9% respectively) values obtained were at least comparable or better than most currently available commercial systems (45). The optimal conditions here defined through this study will now form the technical specifications for the ‘clinical grade’ p-BNC.

The ‘clinical grade’ p-BNC retains identical microfluidic elements and most importantly, the programmable agarose microbead core, permitting rapid and rigorous optimization to be translated for widespread distribution and testing (Fig. 2A). This credit-card-sized p-BNC can interface with and has co-evolved along with a compact (13.5 lbs) toaster size analyzer (Fig. 1) developed by our commercial partners which utilizes Light-Emitting Diode (LED) based optics along with a miniaturized Charge-Coupled Device (CCD) and a mechanical actuator that circumvent the need for a microscope and external pumps, as necessitated for a POC setup (36). In the completely integrated p-BNC (Fig. 2A, III), the loaded sample is accurately metered via a sample loop, following which the card is inserted into the battery-powered analyzer. Here, buffer containing blister packs are crushed and sample and reagents are released by actuation of a stepper motor and delivered to the nano-porous agarose beads housed in a stainless steel chip for assay sequence completion. Biohazardous wastes are contained in the waste chambers housed on the p-BNC. Upon assay completion, optical signal capture followed by automated image analysis results in an output displayed on the built-in screen (37). Lack of such co-developed scaled instrumentation has been a limiting factor for similar high performance microfluidic systems to be distributed in the clinical

settings and adapted to the POC (46), and this potential to untether from expensive traditional laboratory infrastructure is a particularly distinguishing feature of the p-BNC.

The high quality analytical performance here reported for the p-BNC is achieved within 43 minutes, well suited for POC adaptation, permitted by the high surface area and capture efficiency of the 3D agarose nano-fibers compared to the traditional 2D platforms (47). Also, methods such as the p-BNC, circumvent the need for centralized laboratory infrastructure necessitated by ELISA, where turnaround times on the order of 24-48 hours are typical with three degrees of separation between the patient and the results (37). Traditional systems are further limited by one-marker-at-a-time approach and infeasibility for POC adaptation. Further reductions in assay times and sample volumes are anticipated with higher analyte capture efficiency permitted by optimal bead holder chip geometry design powered by computational fluid dynamics.

Method validation of the p-BNC utilizing advanced stage ovarian cancer patient sera demonstrated good correlation ($R^2 = 0.97$) with the current gold-standard ELISA systems (Fig. 6B). To demonstrate proof-of-concept, serum (as utilized in current systems) was chosen. To minimize sample processing and to facilitate POC analysis, we are now investigating the feasibility of whole blood samples obtained from a finger-stick to be applied directly to the p-BNC via capillary loading. Future work will encompass diseased samples at early and pre-clinical stages with corresponding age matched negative controls to encompass the low biomarker concentration range.

This work serves to define from a methods development perspective, the initial implementation of a chip-based ensemble for ovarian cancer biomarker testing at the point-of-care. Further work is required to secure regulatory approval, a necessary and critical step before widespread clinical distribution is possible. Thus, given the preliminary nature of this work, it would be premature to claim full clinical utility for early disease detection at this stage. However, the CA125 p-BNC could envision utility in a variety of scenarios. In this context, CA125 continues to be the single-best biomarker for ovarian cancer despite the search for novel markers (48). High analytical precision permitted by the CA125 p-BNC will enable interpretation of biological variations unconfounded by analytical variations, necessary for MMS. Poor assay precision translates into poor biomarker performance and these results are important in the light of high degree of variation in biomarker assay precision (2% to 58%) noted recently (48). Additionally, CA125 results obtained in 43 minutes can essentially permit TVS (if required) on the same day, pre-empting follow-up visits. Harnessing the multiplexing ability of the p-BNC, consistent with the MMP approach, we are currently placing newly discovered markers on to the p-BNC alongside CA125 for increased PPV (31). Such a system could be utilized for longitudinal monitoring of multiple markers as a potential screening modality. Finally, the CA125 p-BNC could potentially reduce the residence time in the ‘diagnostic pipeline’ paradigm by validating novel biomarkers on the system along with serving as the end-point diagnostic (23).

Taken together, the CA125 p-BNC shows promising utility for ovarian cancer diagnostics, with competitive analytical performance metrics, reduced assay time, potential for multiplexing and POC amenability, necessary for large scale implementation of early detection and screening methodologies.

Supplementary Material

Refer to Web version on PubMed Central for supplementary material.

Acknowledgments

Financial Support

Funding for this work was provided the Cancer Prevention and Research Institute of Texas (CPRIT) as well as by National Institutes of Health (NIH) through the National Institute of Dental and Craniofacial Research (U01 DE015017 and U01 DE017793). The content is solely the responsibility of the authors and does not necessarily represent or reflect views of CPRIT, the NIH or the United States Government. This work was also supported by funds from the National Cancer Institute (NCI) Ovarian SPORE (P5O CA 83639) and philanthropic support from Golfers against Cancer, the Tracey Jo Wilson Foundation and the Mossy Foundation.

The costs of publication of this article were defrayed in part by the payment of page charges. The article must therefore be hereby marked *advertisement* in accordance with 18 U.S.C. Section 1734 solely to indicate this fact.

References

1. Jemal A, Siegel R, Xu J, Ward E. Cancer Statistics, 2010. CA Cancer J Clin.
2. Badgwell D, Bast RC Jr. Early detection of ovarian cancer. Dis Markers. 2007; 23:397–410. [PubMed: 18057523]
3. Urban N, Drescher C. Potential and limitations in early diagnosis of ovarian cancer. Adv Exp Med Biol. 2008; 622:3–14. [PubMed: 18546614]
4. Coticchia CM, Yang J, Moses MA. Ovarian cancer biomarkers: current options and future promise. J Natl Compr Canc Netw. 2008; 6:795–802. [PubMed: 18926090]
5. Kohn EC, Azad N, Annunziata C, Dhamoon AS, Whiteley G. Proteomics as a tool for biomarker discovery. Dis Markers. 2007; 23:411–7. [PubMed: 18057524]
6. Walsh CS, Karlan BY. Contemporary progress in ovarian cancer screening. Curr Oncol Rep. 2007; 9:485–93. [PubMed: 17991357]
7. Urban N. Specific keynote: ovarian cancer risk assessment and the potential for early detection. Gynecol Oncol. 2003; 88:S75–9. discussion S80-3. [PubMed: 12586091]
8. van Nagell JR Jr. DePriest PD, Reedy MB, Gallion HH, Ueland FR, Pavlik EJ, et al. The efficacy of transvaginal sonographic screening in asymptomatic women at risk for ovarian cancer. Gynecol Oncol. 2000; 77:350–6. [PubMed: 10831341]
9. Wang Y, Cheon DJ, Lu Z, Cunningham SL, Chen CM, Luo RZ, et al. MUC16 expression during embryogenesis, in adult tissues, and ovarian cancer in the mouse. Differentiation. 2008; 76:1081–92. [PubMed: 18637025]
10. McLemore MR, Aouizerat B. Introducing the MUC16 gene: implications for prevention and early detection in epithelial ovarian cancer. Biol Res Nurs. 2005; 6:262–7. [PubMed: 15788735]
11. Gogoi R, Srinivasan S, Fishman DA. Progress in biomarker discovery for diagnostic testing in epithelial ovarian cancer. Expert Rev Mol Diagn. 2006; 6:627–37. [PubMed: 16824035]
12. O'Brien TJ, Beard JB, Underwood LJ, Dennis RA, Santin AD, York L. The CA 125 gene: an extracellular superstructure dominated by repeat sequences. Tumour Biol. 2001; 22:348–66. [PubMed: 11786729]
13. Karlan BY, McIntosh M. The quest for ovarian cancer's Holy Grail: can CA-125 still be the chalice of early detection? J Clin Oncol. 2007; 25:1303–4. [PubMed: 17416848]
14. Sturgeon CM, Duffy MJ, Stenman UH, Lilja H, Brunner N, Chan DW, et al. National Academy of Clinical Biochemistry laboratory medicine practice guidelines for use of tumor markers in testicular, prostate, colorectal, breast, and ovarian cancers. Clin Chem. 2008; 54:e11–79. [PubMed: 19042984]
15. Bast RC Jr. Urban N, Shridhar V, Smith D, Zhang Z, Skates S, et al. Early detection of ovarian cancer: promise and reality. Cancer Treat Res. 2002; 107:61–97. [PubMed: 11775462]
16. Skates SJ, Xu FJ, Yu YH, Sjovall K, Einhorn N, Chang Y, et al. Toward an optimal algorithm for ovarian cancer screening with longitudinal tumor markers. Cancer. 1995; 76:2004–10. [PubMed: 8634992]
17. Rosenthal AN, Menon U, Jacobs IJ. Screening for ovarian cancer. Clin Obstet Gynecol. 2006; 49:433–47. [PubMed: 16885651]

18. Menon U, Skates SJ, Lewis S, Rosenthal AN, Rufford B, Sibley K, et al. Prospective study using the risk of ovarian cancer algorithm to screen for ovarian cancer. J Clin Oncol. 2005; 23:7919–26. [PubMed: 16258091]
19. Menon U, Gentry-Maharaj A, Hallett R, Ryan A, Burnell M, Sharma A, et al. Sensitivity and specificity of multimodal and ultrasound screening for ovarian cancer, and stage distribution of detected cancers: results of the prevalence screen of the UK Collaborative Trial of Ovarian Cancer Screening (UKCTOCS). Lancet Oncol. 2009; 10:327–40. [PubMed: 19282241]
20. Zhang Z, Yu Y, Xu F, Berchuck A, van Haaften-Day C, Havrilesky LJ, et al. Combining multiple serum tumor markers improves detection of stage I epithelial ovarian cancer. Gynecol Oncol. 2007; 107:526–31. [PubMed: 17920110]
21. Visintin I, Feng Z, Longton G, Ward DC, Alvero AB, Lai Y, et al. Diagnostic markers for early detection of ovarian cancer. Clin Cancer Res. 2008; 14:1065–72. [PubMed: 18258665]
22. Bandera CA, Ye B, Mok SC. New technologies for the identification of markers for early detection of ovarian cancer. Curr Opin Obstet Gynecol. 2003; 15:51–5. [PubMed: 12544502]
23. Ye B, Gagnon A, Mok SC. Recent technical strategies to identify diagnostic biomarkers for ovarian cancer. Expert Rev Proteomics. 2007; 4:121–31. [PubMed: 17288520]
24. Nossov V, Amneus M, Su F, Lang J, Janco JM, Reddy ST, et al. The early detection of ovarian cancer: from traditional methods to proteomics. Can we really do better than serum CA-125? Am J Obstet Gynecol. 2008; 199:215–23.
25. Yurkovetsky ZR, Linkov FY, D EM, Lokshin AE. Multiple biomarker panels for early detection of ovarian cancer. Future Oncol. 2006; 2:733–41. [PubMed: 17155900]
26. Nosov V, Su F, Amneus M, Birrer M, Robins T, Kotlerman J, et al. Validation of serum biomarkers for detection of early-stage ovarian cancer. Am J Obstet Gynecol. 2009; 200:639 e1–5. [PubMed: 19285648]
27. Bast RC Jr. Badgwell D, Lu Z, Marquez R, Rosen D, Liu J, et al. New tumor markers: CA125 and beyond. Int J Gynecol Cancer. 2005; 15(Suppl 3):274–81. [PubMed: 16343244]
28. Tuxen MK, Soletormos G, Dombernowsky P. Serum tumour marker CA 125 in monitoring of ovarian cancer during first-line chemotherapy. Br J Cancer. 2001; 84:1301–7. [PubMed: 11355938]
29. Soper SA, Brown K, Ellington A, Frazier B, Garcia-Manero G, Gau V, et al. Point-of-care biosensor systems for cancer diagnostics/prognostics. Biosens Bioelectron. 2006; 21:1932–42. [PubMed: 16473506]
30. Rasooly A. Moving biosensors to point-of-care cancer diagnostics. Biosens Bioelectron. 2006; 21:1847–50. [PubMed: 16556495]
31. Yurkovetsky Z, Skates S, Lomakin A, Nolen B, Pulsipher T, Modugno F, et al. Development of a multimarker assay for early detection of ovarian cancer. J Clin Oncol. 28:2159–66. [PubMed: 20368574]
32. Whitesides GM. The origins and the future of microfluidics. Nature. 2006; 442:368–73. [PubMed: 16871203]
33. Mukhopadhyay R. Microfluidics: on the slope of enlightenment. Anal Chem. 2009; 81:4169–73. [PubMed: 19422188]
34. Chin CD, Linder V, Sia SK. Lab-on-a-chip devices for global health: past studies and future opportunities. Lab Chip. 2007; 7:41–57. [PubMed: 17180204]
35. Myers FB, Lee LP. Innovations in optical microfluidic technologies for point-of-care diagnostics. Lab Chip. 2008; 8:2015–31. [PubMed: 19023464]
36. Jokerst JV, Jacobson JW, Bhagwandin BD, Floriano PN, Christodoulides N, McDevitt JT. Programmable nano-bio-chip sensors: analytical meets clinical. Anal Chem. 2010; 82:1571–9. [PubMed: 20128622]
37. Jokerst JV, McDevitt JT. Programmable nano-bio-chips: multifunctional clinical tools for use at the point-of-care. Nanomedicine (Lond). 2010; 5:143–55. [PubMed: 20025471]
38. Jokerst JV, Chou J, Camp JP, Wong J, Lennart A, Pollard AA, et al. Location of biomarkers and reagents within agarose beads of a programmable bio-nano-chip. Small. 2011; 7:613–24. [PubMed: 21290601]

39. Nustad K, Bast RC Jr. Brien TJ, Nilsson O, Seguin P, Suresh MR, et al. International Society for Oncodevelopmental Biology and Medicine. Specificity and affinity of 26 monoclonal antibodies against the CA 125 antigen: first report from the ISOBM TD-1 workshop. Tumour Biol. 1996; 17:196–219. [PubMed: 8685601]
40. Scholler N, Crawford M, Sato A, Drescher CW, O'Briant KC, Kiviat N, et al. Bead-based ELISA for validation of ovarian cancer early detection markers. Clin Cancer Res. 2006; 12:2117–24. [PubMed: 16609024]
41. Paek SH, Schramm W. Modeling of immunosensors under nonequilibrium conditions. I. Mathematic modeling of performance characteristics. Anal Biochem. 1991; 196:319–25. [PubMed: 1776681]
42. Parsa H, Chin CD, Mongkolwisetwara P, Lee BW, Wang JJ, Sia SK. Effect of volume- and time-based constraints on capture of analytes in microfluidic heterogeneous immunoassays. Lab Chip. 2008; 8:2062–70. [PubMed: 19023469]
43. Thompson JA, Bau HH. Microfluidic, bead-based assay: Theory and experiments. J Chromatogr B Analyt Technol Biomed Life Sci. 2010; 878:228–36.
44. Zimmermann M, Delamarche E, Wolf M, Hunziker P. Modeling and optimization of high-sensitivity, low-volume microfluidic-based surface immunoassays. Biomed Microdevices. 2005; 7:99–110. [PubMed: 15940422]
45. Mongia SK, Rawlins ML, Owen WE, Roberts WL. Performance characteristics of seven automated CA 125 assays. Am J Clin Pathol. 2006; 125:921–7. [PubMed: 16690492]
46. Sia SK, Kricka LJ. Microfluidics and point-of-care testing. Lab Chip. 2008; 8:1982–3. [PubMed: 19023459]
47. Jokerst JV, Chou J, Camp JP, Wong J, Lennart A, Pollard AA, et al. Location of biomarkers and reagents within agarose beads of a programmable bio-nano-chip. Small. 7:613–24. [PubMed: 21290601]
48. Cramer DW, Bast RC Jr. Berg CD, Diamandis EP, Godwin AK, Hartge P, et al. Ovarian cancer biomarker performance in prostate, lung, colorectal, and ovarian cancer screening trial specimens. Cancer Prev Res (Phila). 4:365–74. [PubMed: 21372036]

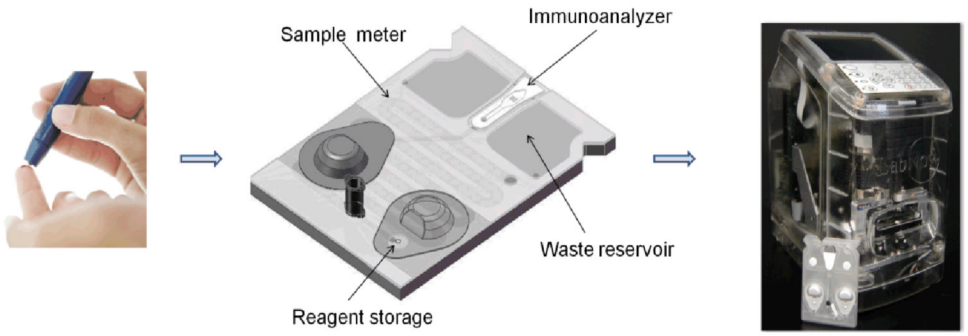

Fig. 1.

Illustration of the envisioned POC use of the p-BNC for early detection and screening of ovarian cancer. Sample is obtained from the patient via venipuncture (serum) or finger-stick (left) and transferred to the p-BNC card (center) for analysis. The p-BNC card houses a miniaturized microbead immunoanalyzer with on-card sample metering, reagent storage and biohazard waste disposal. Following sample introduction, the p-BNC card is loaded into the battery-powered analyzer (right) possessing mechanical, optical and electronic components to drive the single analyte or multimarker panel immunoassays to completion, followed by automated imaging, analysis and readouts for access by the clinician.

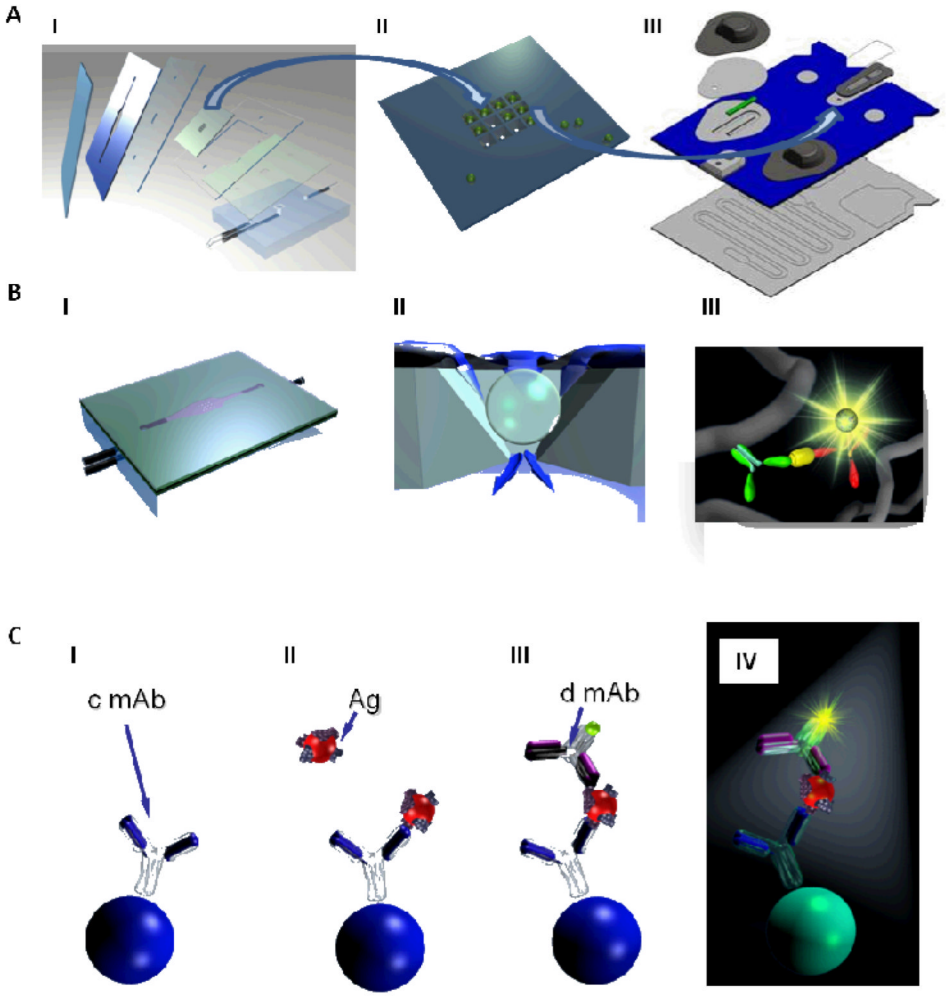

Fig. 2.

The research grade (A, I) and the completely integrated p-BNC (A, III) retain identical microbead immunoanalyzers housed in a bead holder (A, II) permitting optimization of individual components and translation between the systems. The p-BNC houses the microchip (A, II) and is constructed with alternate layers of precision cut double sided adhesive and laminates to generate microfluidic features (A, I, III). Reagents and sample are uniformly delivered to the agarose microbeads (B, II) and sandwich immunoassays are completed in the agarose nano-nets (B, III). Immunoschematic illustration (C, I-IV) depicts sequential molecular events on the agarose microbead immobilized with capturing antibody (c mAb) specific to the analyte of interest (C, I), introduction of sample containing analyte (Ag) of interest followed by binding to the cmAb (C, II), formation of a completed immuno-molecular sandwich (C, III) with analyte-specific Alexa Fluor® 488 coupled detecting antibody (d mAb) and signal visualization with fluorophore excitation (C, IV) where the generated signal is proportional to the analyte concentration. Unbound analyte and detecting antibody are removed with high stringency washes following steps II and III (not depicted).

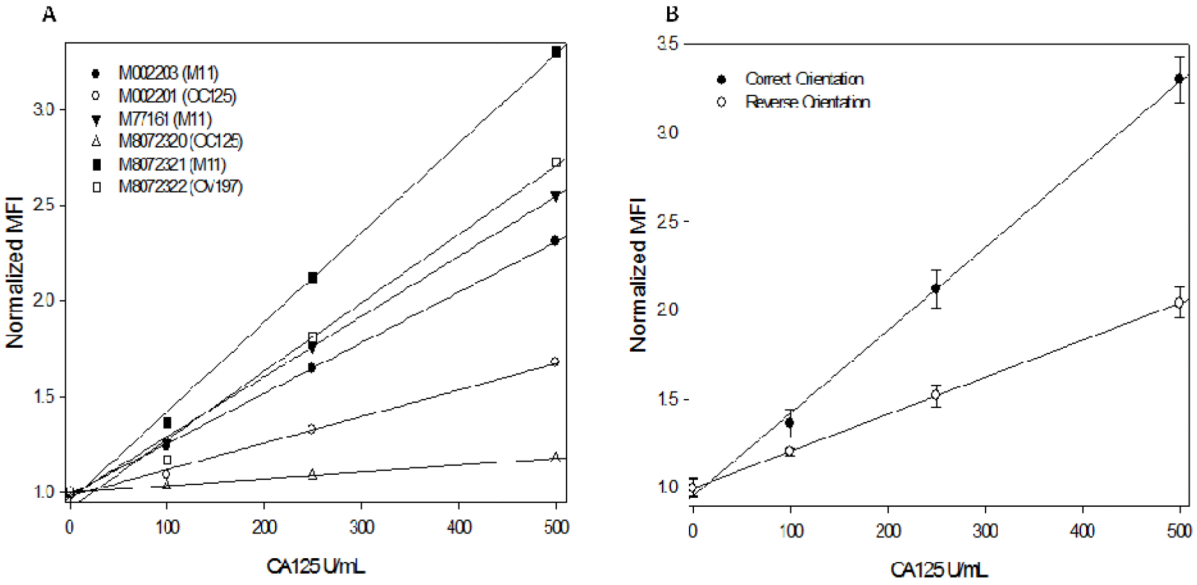

Fig. 3.

(A) Calibration curves for a series of antibody pair combinations generated with clone M8072320 (OC125) as the detecting antibody and the clones shown in the legend as capturing antibodies. The optimal matched pair (clone M8072321 as the capturing antibody and M8072320 as the detecting antibody) was chosen based on the highest slope exhibited by the corresponding calibration curve. The performance gradient of the various antibodies was concordant with their associated epitope specificities. (B) Calibration curves demonstrating the importance of matched pair orientation in a flow based immunosensor system. Here, the correct orientation with clone M8072321 as the capturing moiety (and M8072320 as the detecting antibody) exhibited significantly higher performance in terms of slope and SNR in comparison with the reversed orientation where the same clone was utilized for detection.

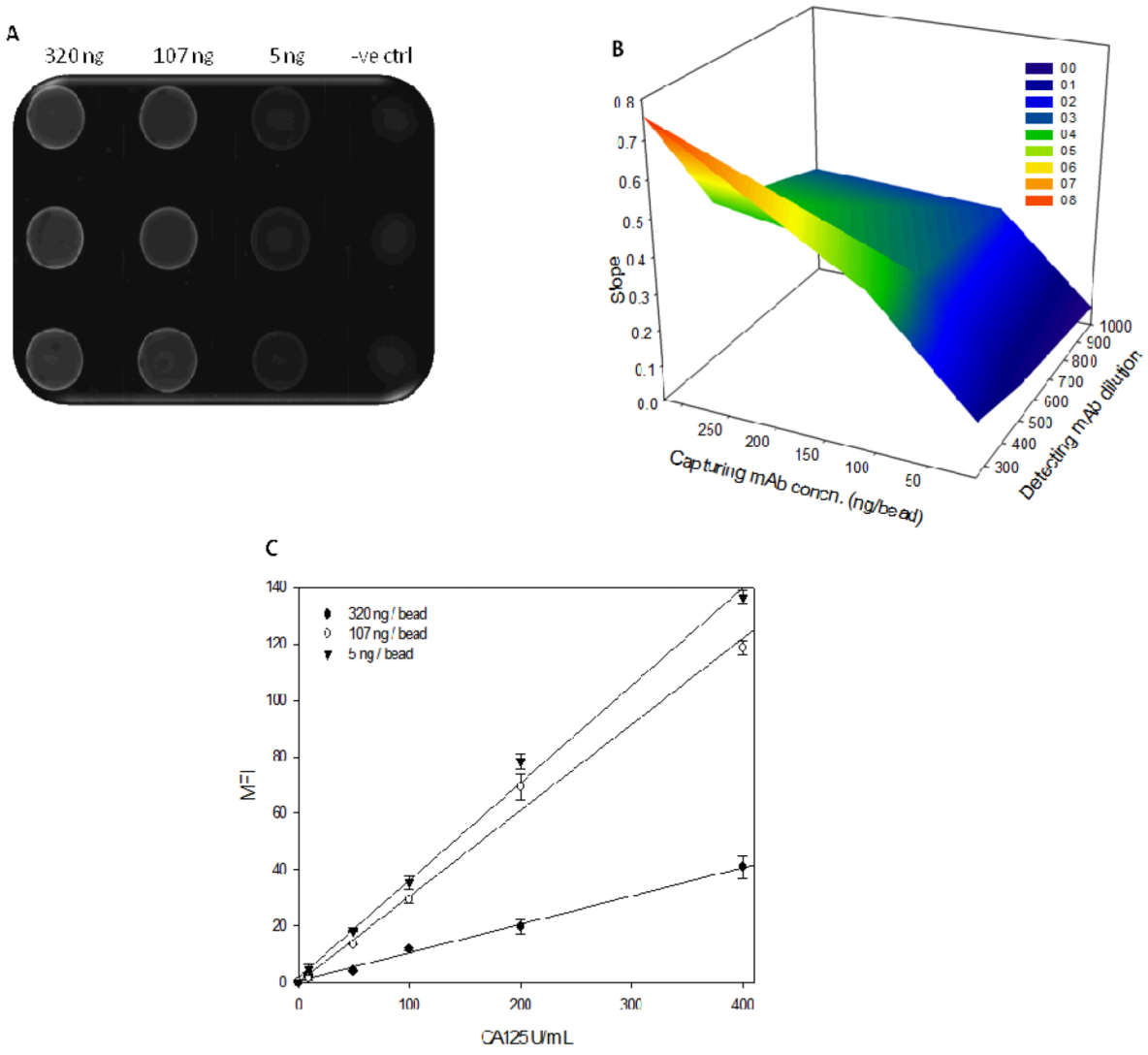

Fig. 4.

(A) Typical photomicrograph demonstrating advantages of the p-BNC immunosensor to simultaneously assess multiple capturing antibody concentrations in one experimental run. (B) A 3-dimensional surface plot demonstrating influence of capturing and detecting antibody concentrations on the slope of the resultant immunoassay. The highest slope is seen for the capturing and detecting antibody concentration combination corresponding to the peak denoted by the orange zone (See legend). (C) Calibration curves demonstrating the effect of capturing antibody concentration on the slope of the CA125 immunoassay with higher concentrations demonstrating increased slope at the detecting antibody dilution exhibiting the highest linearity.

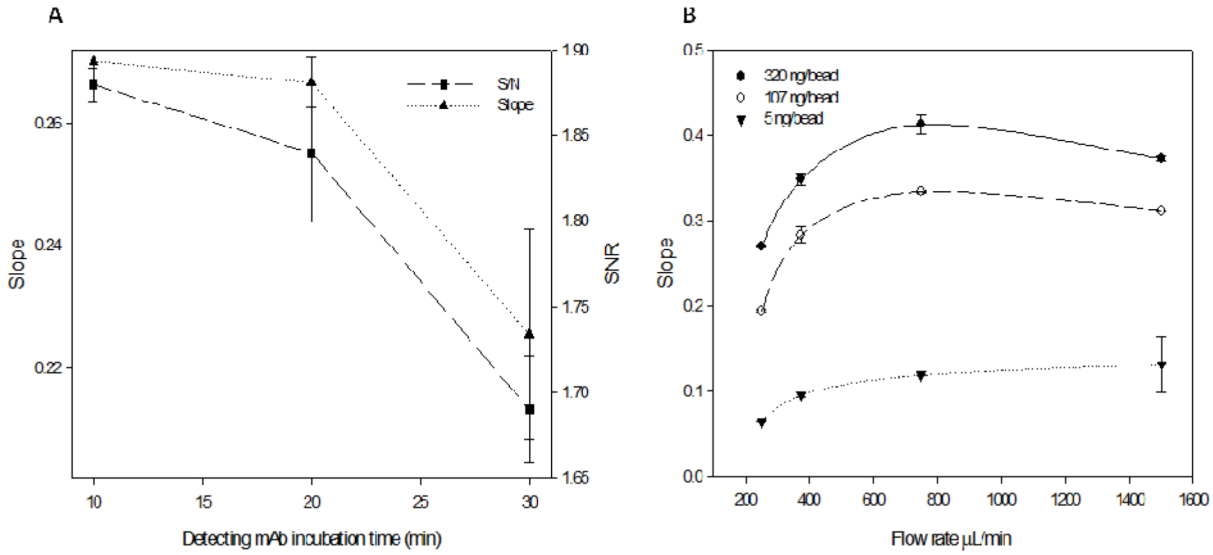

Fig. 5.

(A) Effect of detecting antibody incubation times on the slope and SNR of the CA125 p-BNC. Decrease in incubation time resulted in improved immunoassay slope along with corresponding increase in precision demonstrated by the error bars. (B) Effect of sample incubation flow rates on the slope of the CA 125 immunoassay. Initial increase in flow rate resulted in a steep increase in slope through 750 µL/min (optimal flow rate) for the optimal capturing antibody concentration (320 ng/bead) and then leveled off. Similar trends were also noted for other capturing antibody concentrations.

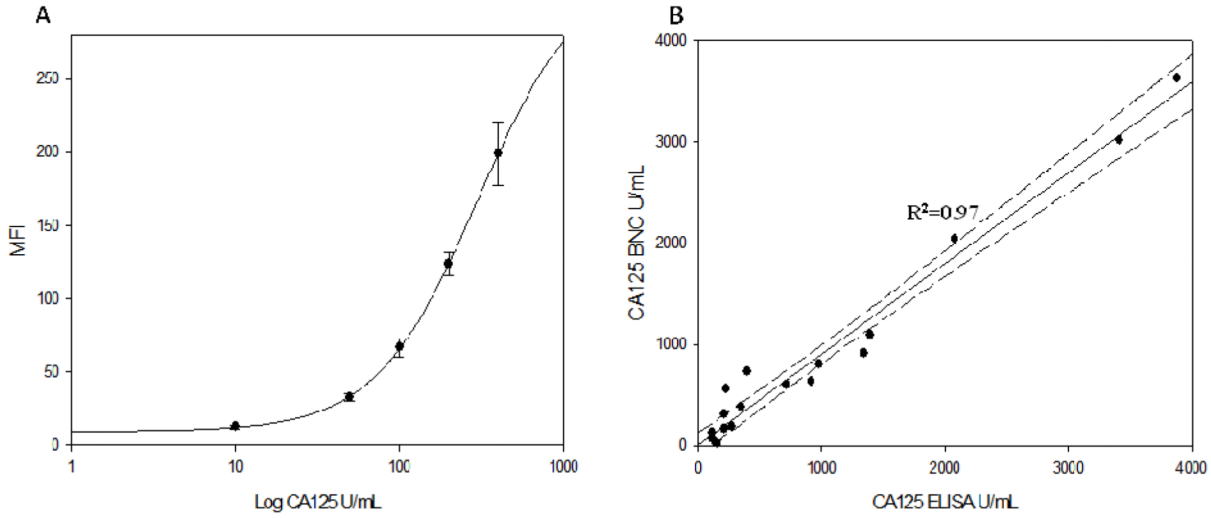

Fig. 6.

(A) Dose-response curve for CA125 quantification on the p-BNC over 10-400 U/mL concentration range. (B) Plot demonstrating good correlation between the p-BNC and FDA approved ELISA for values of CA125 measured in the sera of advanced stage epithelial ovarian cancer patients.

Table 1

Effect of each optimization step on the LOD and the corresponding linearity and precision. Results indicate improvement in LOD and precision for each optimization step with the most improvement noted for the sample incubation flow rate step.

Optimization step	LOD (U/mL)	Linearity	Avg %CV
Matched pair identification	35.1[#]	0.9982	5.04
⬇			
Detecting mAb concentration	4.75	0.9999	3.69
⬇			
Capturing mAb concentration	4.33	0.9952	2.92
⬇			
Detecting mAb incubation time	2.71	0.9930	4.26
⬇			
Sample incubation flow rate	0.24	0.9980	2.09
⬇			
Optimized assay	0.24	0.9980	2.09